

Protein dynamics without energy landscape: a molecular model based on elastic and time domain neutron scattering

Wolfgang Doster

Technical University Munich, Physics Department and FRM 2 Garching, Germany

Submitted to Proceedings of the National Academy of Sciences of the United States of America

The first elastic-inelastic neutron scattering experiments, performed with hydrated myoglobin in 1989¹, created a new approach to protein dynamics and molecular simulations by opening the temperature range. The goal was to separate different kinds of motion including low temperatures by thermally stable hydrated powders instead of solutions². Two dynamic transition temperatures were identified by the abrupt enhancement of hydrogen displacements at 150 K and 240, which was interpreted as the onset of rotational jumps of side chains and water-coupled translational motions^{1,3}. Today, after 30 years of effort, combining experiments with computer simulations, there is still no accepted molecular model of protein structural fluctuations⁴⁻¹⁰. Instead, phenomenological descriptions of dynamical heterogeneity are forcefully promoted such as complex energy landscapes and the softening of protein force constants⁶⁻¹⁰. This approach ignores the potential of neutron scattering to provide molecular insight. We propose a model of minimal complexity comprising the original two basic types of molecular motions. The model density correlation function of hydrogen fluctuations reproduces the combined elastic-inelastic neutron scattering experiments within a wide range of time scales, momentum exchange and temperature. Protein fluctuations are studied in the time domain versus temperature without the need to focus on dynamical transitions. In this effective description of protein dynamics heterogeneity plays only a minor role.

bioneutron scattering | protein dynamics | hydration water | methyl rotation | energy landscapes

1) Introduction: hydrogen fluctuations

Hydrogens constitute nearly half of the atoms in proteins. They mediate hydrogen bridges in helices and take part in other nonbonding interactions of electrostatic and van der Waals forces. Polar bonds play a critical role in enzyme catalysis, substrate binding and proton transfer reactions. Main chain and side chain hydrogens contribute to the stability of the protein secondary structure and mediate structural fluctuations. Neutron diffraction provides a more precise determination of hydrogen positions and fluctuation amplitudes than x-ray crystallography, because the hydrogen cross section is comparable to those of C, N and O¹¹. A particularly useful property of the proton is its large incoherent cross section, about ten times above those of other atoms. 85 % of protein incoherent scattering results from hydrogens¹². Incoherent dynamic neutron scattering is a unique tool to record time resolved the average displacements of single hydrogen atoms on a sub-nanosecond time scale^{3,14}: The scattering contribution of hydration water in the powder can be kept as low as 4 % with D₂O¹². Energy resolved spectra, Fourier-transformed to the time domain, yield a hydrogen weighted density correlation function of structural fluctuations. The first inelastic experiments performed at subzero temperatures were published in 1989 with dry and hydrated myoglobin, which created a new approach to protein dynamics on a picosecond time scale¹. The goal was to separate different kinds of motion by their temperature depen-

dence using thermally stable D₂O- hydrated powders instead of solutions. Another advantage of low hydration is to arrest global diffusion, emphasizing the spectral contribution of internal structural fluctuations, while hydrated proteins as in crystals are still functional. Elastic scans versus the temperature revealed two dynamical transitions by the abrupt enhancement of hydrogen displacements above 150 K and 240 K. They were assigned to rotational motions of side chains and water-coupled translational displacements^{1,3}. These experiments also stimulated a large number of low temperature MD simulations with proteins, which is now a well-established procedure¹³.

Today, after 30 years of effort combining neutron scattering experiments with computer simulations, there is still no accepted molecular model of protein motions³⁻¹⁰. Our initial two-component molecular approach was discarded. Instead, phenomenological descriptions dominate, such as 'complex energy landscapes'^{8,9}, dynamical heterogeneity distributions^{6,7} and the softening of overall protein force constants¹⁰. The phenomenological approach ignores the potential of neutron scattering to provide molecular insight complementary to simulations. We propose a model of minimal complexity, comprising the original two basic types of molecular motions, which is shown to account for the complete elastic-inelastic data set of hydrated and dry myoglobin. Similar data exist for other hydrated proteins.

The main experimental quantity to be determined is the density self-correlation function $G_s(\vec{r}, t)$ characterizing the distribution of single particle displacements \vec{r} within time t . For isotropic powder samples only the magnitude of \vec{r} matters. In scattering

Significance

Despite a combined theoretical and experimental effort for 30 years there is still no accepted model of molecular motions in proteins. The molecular approach has been largely replaced by phenomenological models such as energy landscapes, global force constants and dynamic heterogeneity. We present a minimal molecular model of hydrogen fluctuations in proteins, which reproduced both elastic and inelastic neutron scattering data covering a wide range of time scales, momentum exchange and temperature. Such an effective molecular description helps to understand the role of specific motions in protein function. It is also shown, why neutron scattering spectra are not heterogeneous as postulated in a series of papers in PNAS by Frauenfelder et al.

Reserved for Publication Footnotes

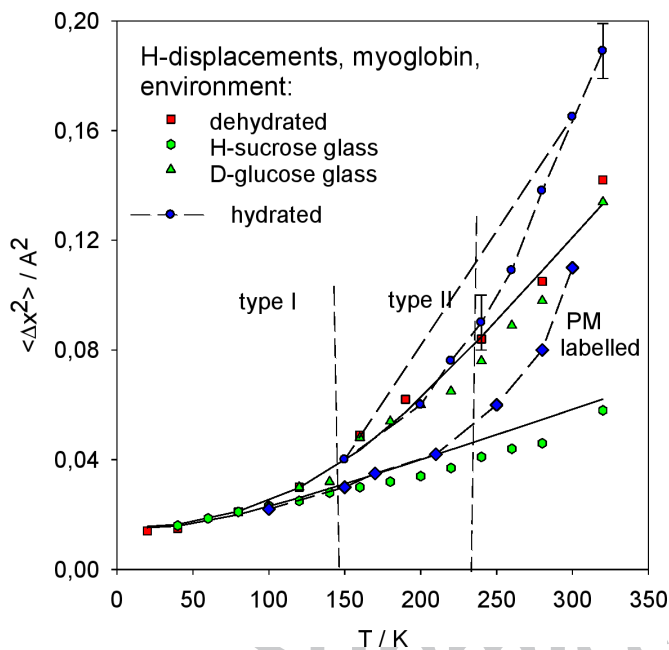


Fig. 1. mean square displacements (IN13, $\tau_{res} = 140$ ps) of myoglobin in various environments: dehydrated (red squares), hydrated (blue circles), green triangles: per-deuterated glucose glass, green circles: DI H-sucrose glass^{10,2}, blue diamonds: H-labelled per-deuterated PM fragments¹⁰, line: calculated f vibrational displacements¹⁶. The onset temperatures at 150 K (I) and 240 K (II) are indicated.

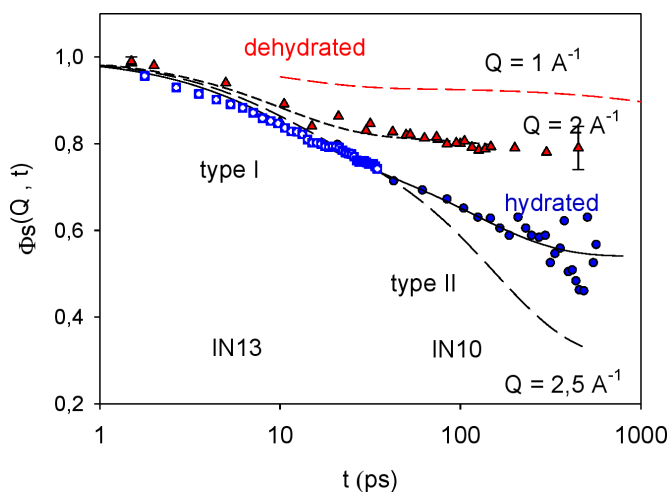


Fig. 2. Wide range density correlation function of dry and hydrated myoglobin at 300 K and $Q = 2 \text{ \AA}^{-1}$, combining the spectral information of two instruments, IN13 (squares) and IN10 (full circles). Full line: fits to equ.3-5 adjusting the time constants, $\tau_{rot} = 10 (\pm 1)$ ps, $\tau_{trans} = 145 (\pm 10)$ ps and $\delta^2 = 0,11 (\pm 0,015) \text{ \AA}^2$. Dashed lines: effect of different Q -values.

experiments one measures the intermediate scattering function in momentum-space, which is the Fourier transform of the density correlation function^{14,15}:

$$\Phi_s(Q, t) = \langle \int d^3r \cdot e^{-iQ \cdot r} G_s(\vec{r}, t) \rangle_{powder} \quad (1)$$

The resulting powder averaged intermediate scattering function $\Phi_s(Q, t)$ of N protein sites has the following structure^{2,15}:

$$\Phi_s(Q, t) = \frac{1}{N} \sum_i \Phi_i(Q, t) = \frac{1}{N} \sum_i \exp \left[-Q^2 \langle \Delta x_i^2(t) \rangle / 2 + Q^4 \dots \right] \quad (2)$$

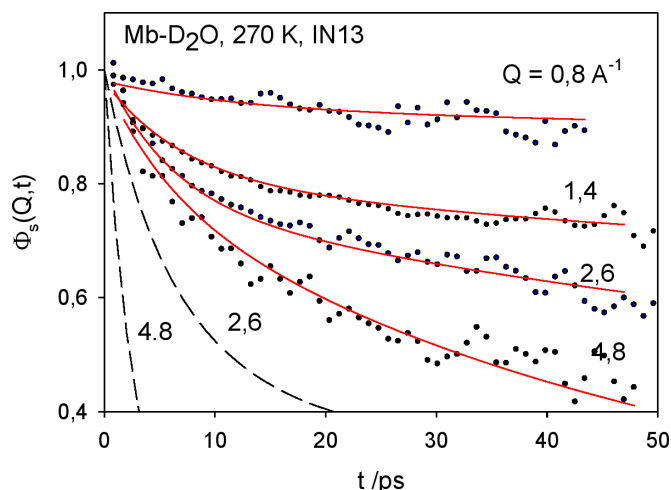


Fig. 3. Time domain density correlation function $\Phi_s(Q, t)$ of myoglobin- D_2O (0,35 g/g) derived from spectral data of the back-scattering spectrometer IN13 at various Q values. The red lines are the predictions of the TR model with $\delta^2 = 0,11 (\pm 0,02) \text{ \AA}^2$, $\tau_{rot} \approx 11 (\pm 2) \text{ ps}$ and $\tau_{trans} \approx 155 (\pm 20) \text{ ps}$ at 270 K. The dashed lines are the predictions of the Brownian oscillator of equ.5.

where Q is the magnitude of the scattering vector, $Q = 4\pi / \lambda \sin(\theta / 2)$, λ denotes the incoming neutron wavelength and θ is the scattering angle relative to the incident direction. Equ. 2 defines the moment expansion of the hydrogen displacement distribution $G_s(r, t)$, with $\langle \Delta x_i^2(t) \rangle$ as the mean square displacement (MSD) of a specific site 'i' at time t . Expanding $\Phi_s(Q \rightarrow 0, t)$ in the "Gaussian" approximation yields the site averaged MSD: $\langle \Delta x^2 \rangle_t = \sum \langle \Delta x_i^2 \rangle / N$. Temperature dependent MSD scans were measured for numerous proteins under different environmental conditions. Fig. 1 summarizes some essential results for myoglobin³:

Vibrational displacements are characterized by a linear MSD temperature dependence. A prominent example is provided by myoglobin embedded in a D-exchanged hydrogenated sucrose glass, suggesting that vitrified proteins do not move¹⁰. By contrast, with myoglobin embedded in a fully deuterated glass, D-glucose, a strong nonlinear enhancement of the MSD(T) appears at 150 K².

Surprisingly, dehydrated myoglobin exhibits nearly the same MSD temperature dependence as myoglobin in the deuterated glass³. The type I transition at 150 K is thus attributed to the onset of protein internal motions, which are not sensitive to changes of the protein environment. By contrast, with D_2O -hydrated myoglobin, two transition temperatures at 150 K (type I) and 240 K (type II) are recorded, suggesting two well separated molecular processes. Since the second transition (type II) does not occur without water, these motions were assigned to protein displacements related to a wet protein surface^{1,3}. Since the scattering fraction of hydration water (D_2O) amounts to less than 5 %, type II motions characterize the indirect effect of hydration on structural fluctuations. Experiments performed with "wet" per-deuterated purple membrane fragments yield similar but noisier MSD scans with two transitions at the same temperatures as hydrated myoglobin. By contrast, if the per-deuterated fragments are specifically labelled with protonated, but methyl-free residues, the type I transition is missing, although type II at 240 K is still occurs¹⁰. This implies, that type I displacements reflect mostly the methyl side chains^{3,4}. Then Type II by contrast may involve prominently polar residues near the surface. But an indirect effect of hydration on the mobility of nonpolar, non-methyl side chains cannot be excluded.

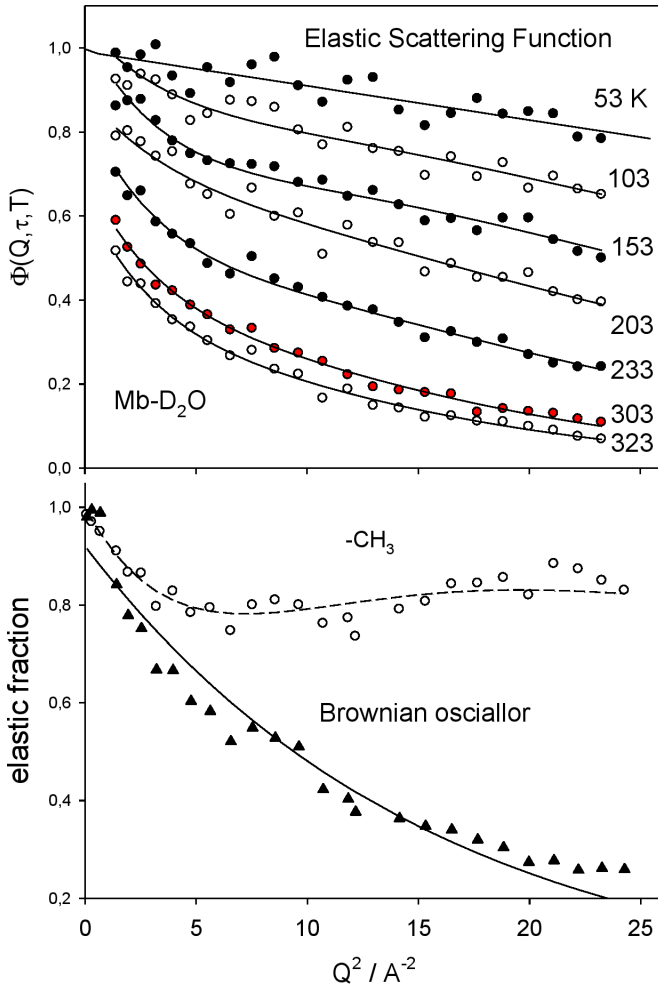


Fig. 4. a): Elastic scattering profiles of hydrated myoglobin (0,35 g/g) normalized at 10 K, back-scattering spectrometer IN13 at $\tau_{res} = 140$ ps and fits to eqs.5-6 by adjusting $\tau_{rot}(T)$ and $\tau_{trans}(T)$ with $\delta^2 = 0,1 \text{ \AA}^2$ kept fixed (full line). b) Decomposition of the elastic scattering functions of hydrated myoglobin at $\tau_{res} = 140$ ps and 270 K according to the TR-model, the full lines are predictions of eqs. 4 and 6.

2. Results

a) Definition of the translation-rotation model (TR).

Based on results in fig. 1, we propose a bimodal distribution of sites associated with two kinds of processes³: (I) internal rotational transitions and translational displacements (II). Process I has been identified with methyl group rotational transitions, while the nature of the second component may be characterized as a localized translational motion. The resulting bimodal correlation function then has the form:

$$\Phi_s(Q, t) = \sigma_I \cdot \Phi_I(Q, t) + (1 - \sigma_I) \cdot \Phi_{II}(Q, t) \quad (3)$$

σ_I denotes the fractional cross section of the type I sites.

Equ. (3) must be complemented by global diffusion at water contents above $h = 0,4$ g/g. According to the neutron structure of myoglobin about 25 % of the total number of hydrogens are organized in methyl groups¹¹, thus $\sigma_I = \sigma_m \cong 0,25$.

More specifically, type I motions are defined by a three site jump model of methyl groups reorienting by 120° jumps about their three-fold symmetry axis^{3,14}:

$$\Phi_{rot}(Q, t) = \frac{1}{3} (1 + 2j_0(Q) + 2 \cdot (1 - j_0(Q)) \cdot \exp(-t/\tau_{rot})) \quad (4)$$

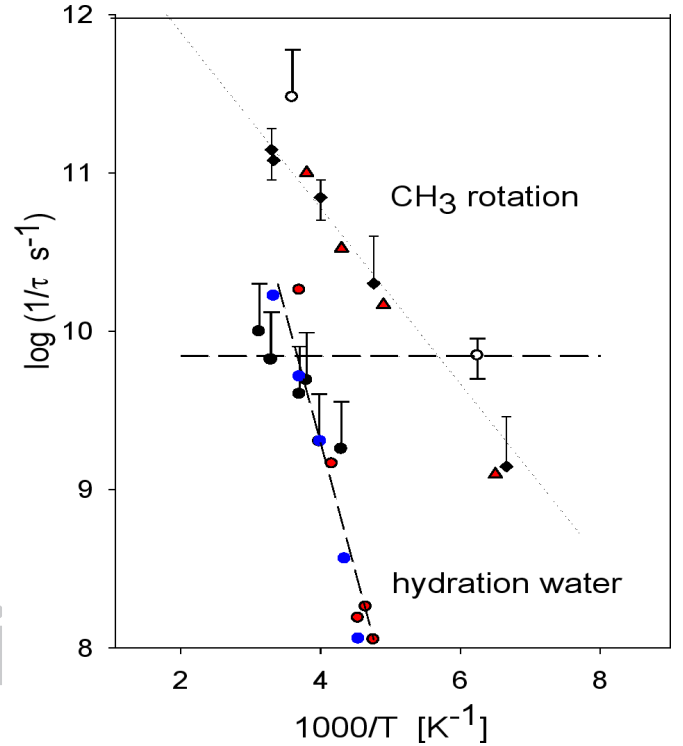


Fig. 5. Arrhenius plot of the fitted correlation times, τ_{rot} : black diamonds: elastic scans, open circles: alanine dipeptide⁵, red triangles: τ_{rot} , from fit of IN6 spectrum of dry myoglobin, τ_{trans} : black circles: elastic scans, blue and red circles: τ_{hyd} , hydration water^{5,19}, dashed line: $\tau_{res} = 140$ ps (Instrument IN13)

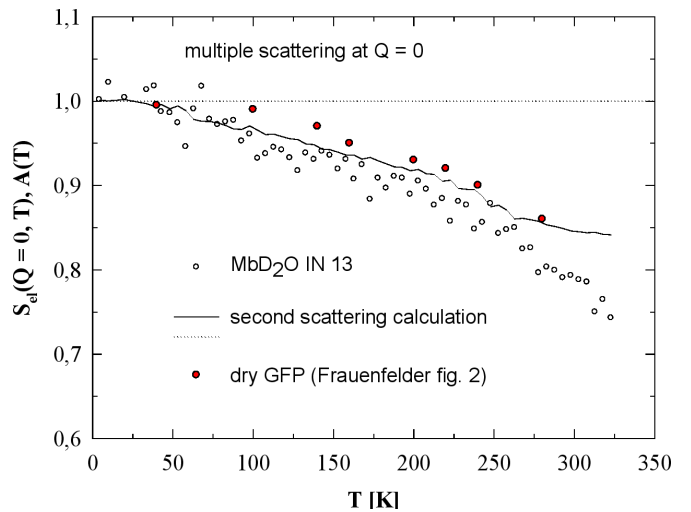


Fig. 6. : elastic intensity $S_{el}(Q=0, T)$ from fits of the data in fig. 4 (open circles) and $A(T)$: calculations of the second scattering intensities (full line), red dots: reconstructed elastic intensities at zero Q of dry GFP by Frauenfelder et al.⁸.

$$j_0(Q) = \sin(Q\sqrt{3} \cdot r) / (Q\sqrt{3} \cdot r)$$

By contrast, type II describes the translational displacement of residues confined by a quasi-harmonic potential, which we approximate by an over-damped Brownian oscillator¹⁷:

$$\Phi_{trans}(Q, t) = \exp[-Q^2 \delta^2 \cdot (1 - \exp(-t/\tau_{trans}))] \quad (5)$$

$\delta^2 = \langle \Delta X^2 \rangle_{\text{trans}}$ denotes the translational mean square displacement, which is apart from the time constants, the main free parameter of the model. At long times,

$\Phi_{\text{trans}}(Q, t \gg \tau_{\text{trans}})$ turns into a Gaussian elastic scattering function:

$$\Phi_{\text{trans}}(Q, t \gg \tau_{\text{trans}}) = \exp(-Q^2 \cdot \delta^2) \quad (6)$$

From now on, eqs. 3 – 5 are denoted as the “TR model”.

b) Time domain analysis of hydrogen fluctuations

The first experimental test of the TR model will be performed with time domain data derived from a combination of two backscattering spectrometers of IN10 and IN13. Fig. 2 compares the experimental and model density correlation function of dry and hydrated myoglobin at $Q \cong 2 \text{ \AA}^{-1}$ on a logarithmic time scale. A single fast process (type I) is observed for the dehydrated case, which settles to a long time plateau around 0,8. Fits with the TR correlation function reproduce the correct plateau value for $Q = 2 \text{ \AA}^{-1}$, with the methyl structure factor and the partial cross section of 0,25 as input. At $Q = 1 \text{ \AA}^{-1}$ a much smaller decay is predicted.

This result is compatible only with the methyl group rotation. A much lower plateau is expected if other side chain or main chain transitions interfere.

The fit yields a rotational correlation time, $\tau_{\text{rot}} = 10 (\pm 2)$ ps.

The barrier to methyl group rotation in proteins is 12 kJ/mol. With a pre-factor of 10^{-13} s one obtains 11 ps consistent with the result above.

In the hydrated case, the same fast component appears, but in addition a second process emerges at much longer times. The full line shows the prediction of the TR model at $Q = 2 \text{ \AA}^{-1}$. The resulting time constants are: $\tau_{\text{rot}} = 10 (\pm 2)$ ps and $\tau_{\text{trans}} = 140 (\pm 15)$ ps. This result confirms the MSD analysis of fig. 1 with two well separated onset temperatures. For a slightly larger Q at 2.5 \AA^{-1} , a much too strong decay is obtained, which illustrates the sensitivity of the method.

c) Displacement distribution from momentum exchange experiments

In fig. 3 we present an extended Q-range but slightly reduce the time window, since long times and large Q value are technically not compatible.

The fits with the TR model work quite well using the correlation times determined above as input (fig. 2). The MSD is adjusted, yielding, $\delta^2 = 0,11 (\pm 0,02) \text{ \AA}^2$.

The Brownian oscillator (equ. 5) yields a too strong Q-dependence. This suggests that the spatial displacement distribution is adequately reproduced by the TR model.

d) Elastic backscattering experiments with D₂O-hydrated myoglobin

The IN10 back-scattering spectrometer (ILL, Grenoble)¹⁴ has an energy resolution of $1 \mu\text{eV}$ at $\lambda = 6 \text{ \AA}$, combined with a moderate Q-range up to 2 \AA^{-1} . The IN13 back-scattering spectrometer is famous for its large Q-range up to 5 \AA^{-1} at a resolution of $7 \mu\text{eV}$. Taken together both spectrometers cover a time window of 20 to 600 ps. The elastic intensity was determined using a fixed energy window method ($\tau_{\text{res}} = 140$ ps) with the backscattering spectrometer IN13¹⁴. With 350 mg of hydrated sample the neutron transmission was close to a tolerable 90 %. Raw data were corrected for detector response and cell scattering. The elastic scattering curves, shown in fig. 5a, were normalized at the lowest temperature, but not at each temperature separately. To unravel the dynamic aspects of elastic scattering, we have introduced the method of “elastic resolution spectroscopy”^{5,18}, where the resolution function is varied. In the simplest case of a δ -correlated resolution function⁴, the normalized elastic intensity

versus Q reproduces the time correlation function at fixed time τ_{res} of the spectrometer:

$$S_{\text{el}}^N(Q) \cong \Phi_s(Q, \tau_{\text{res}}) \quad (7)$$

Thus by fitting the elastic scans at fixed time $t = \tau_{\text{res}}$ by adjusting $\tau_{\text{rot}}(T)$ and $\tau_{\text{trans}}(T)$ one derives dynamic information from elastic data. Since we are interested only in average correlation times, we discuss the simplest model here. But fits taking into account the Gaussian resolution function of IN13 have also been performed^{3,5}.

This procedure works reasonably well. The most striking result is the absence of dynamical transitions. The fitted MSD parameter $\delta^2 \cong 0,1 \text{ \AA}^2$ is almost temperature independent.

Equally important, the resulting correlation times $\tau_{\text{rot}}(T)$, displayed in fig. 5, compare well with those determined independently by spectral analysis of dehydrated myoglobin and the methyl side chain of alanine dipeptide⁵.

Finally, the translational correlation times $\tau_{\text{trans}}(T)$ superimpose within experimental error with those derived for hydration water by neutron spectroscopy^{5,19}. This indicates that hydration water and polar protein residues move together on the same time scale by mutual interaction.

e) Multiple scattering

The analysis presented above assumes that each neutron on its passage through the sample is scattered only once. In real experiments at a transmission near 90% about 17 % of the neutrons are scattered at least twice. Although multiple scattering is significant, it is generally ignored. Most significant are elastic-elastic second scattering events due to the large dynamic structure factor of proteins at $\omega = 0$.

Multiple scattering is approximately independent of Q ¹⁶, which produces an extra intensity at $Q = 0$. Since the elastic intensity decreases with temperature increase, multiple scattering also decreases. As a result, one always observes with elastic scans an extra intensity at $Q = 0$, which is temperature dependent: $S_{\text{el}}(Q = 0, T)$. This is why data are usually not only normalized to a low temperature scan but also at each temperature at $Q = 0$ separately. Several examples are given by Frauenfelder et al.⁸. This effect is of course incompatible with single scattering theory, it would violate particle conservation. This discrepancy is now used as a main argument by Frauenfelder et al. to discard conventional scattering theory⁸.

In fig. 6 we display the elastic intensities derived from fits to the TR model of the data presented in fig. 4a), which were extrapolated to $Q = 0$. It shows the effect of a temperature dependent zero Q elastic intensity. Also shown are extensive calculations of the second order scattering for an infinite slab sample based on the theory of Sears¹⁴. The calculated $A(T)$ reproduces the experiment rather well except at high temperatures, where quasi-elastic scattering dominates. Also shown are the reconstructed elastic intensities at zero Q of the green fluorescent protein of Frauenfelder et al.⁸. Given the uncertainties of the extrapolation procedure and the unknown transmission, the agreement is striking. Multiple scattering is thus a valid explanation for the GFP results. Before energy landscapes come into play one has to first correct first for the unavoidable multiple scattering effects.

3. Discussion

I am surprised, how smoothly this minimal TR model can reproduce the complete elastic-inelastic data set of myoglobin, applying well established single scattering theory. The main reason is of course that we use a valid concept and second, one is dealing with two processes, which are well separated in time and Q-space. So there is little space left for alternative interpretations. We have chosen the time domain to show that the postulate of inhomogeneous neutron scattering spectra by Frauenfelder et al. is meaningless. Otherwise we could not have derived time con-

545
546
547
548
549
550
551
552
553
554
555
556
557
558
559
560
561
562
563
564
565
566
567
568
569
570
571
572
573
574
575
576
577
578
579
580
581
582
583
584
585
586
587
588
589
590
591
592
593
594
595
596
597
598
599
600
601
602
603
604
605
606
607
608
609
610
611
612

stants, which are well established in the literature by numerous experiments.

The two kinds of motions of the TR model were identified in earlier functional studies: Flash photolysis experiments of ligand binding to myoglobin reveal, that internal ligand displacements are entirely decoupled from the solvent similar to type I above, this includes even the final binding step of CO to the heme. However, ligand exchange processes across the protein-solvent interface vary with the solvent viscosity similar to type II^{20,21}. Moreover, multiple flash experiments demonstrate, that heterogeneous non-exponential kinetic of ligand binding to myoglobin

1. Doster, W., Cusack, S., Petry, W. Dynamical transition of myoglobin revealed by inelastic neutron scattering. *Nature* **337**, 754-756 (1989)
2. Doster, A., Bachleitner, A., Dunau, R., Hiebl, M., Lüscher, E. Thermal properties of water in myoglobin crystals and solutions at subzero temperatures. *Biophys. J.* **50**, 213-219 (1986)
3. Doster, W., Settles, M., Protein-water displacement distributions. *Biochim. Biophys. Acta.* **1749**, 173-186 (2005)
4. Doster, W., Concepts and misconceptions of the protein dynamical transition, *Eur. Biophys. J.* **37**, 591-602 (2008)
5. Doster, W., Nakagawa, H., Appavou, M.S. Scaling analysis of bio-molecular dynamics derived from elastic neutron scattering experiments. *J. Chem. Phys.* **139**, 45105 -16 (2013)
6. Peters, J., Kneller, G.R., Motional heterogeneity in human acetylcholinesterase revealed by a non-Gaussian model for elastic incoherent neutron scattering. *J. Chem. Phys.* **139**, 165102 1-5 (2013)
7. Vural, D., Hu, X., Lindner, B., Jain, N., Miao, Y., Cheng, X., Liu, Z., Hong, L., Smith, J.C. Quasi-elastic neutron scattering in biology, theory and applications. *Biochim. Biophys. Acta.* **1861**, 3638-3681 (2017)
8. Frauenfelder, H., Young, R. D., Fenimore, P.W. The role of momentum transfer during incoherent neutron scattering is explained by the energy landscape model. *Proc. Natl. Acad. Sci. USA* **114**, 5130-5135 (2017)
9. Frauenfelder, H., Fenimore, P.W., Young, R.D. A wave-mechanical model of incoherent quasi-elastic scattering in complex systems. *PNAS USA* **111**, 12764-12768 (2014).
10. Zaccai, J., How soft is a protein, a protein dynamics force constant measured by neutron scattering. *Science* **288**, 1604-1607 (2000)
11. Engler, N., Ostermann, O., Niimura, N., Parak, F. Hydrogen atoms in proteins: positions and dynamics. *Proc. Natl. Acad. Sci. USA.* **100**, 10243-10248 (2003)
12. Gaspar, A.M., Busch, S., Appavou, M. S., Häußler, W., Georgii, R., Su, Y., Doster, W. Using polarization analysis to separate coherent and incoherent scattering from protein samples, *Biochim. Biophys. Acta.* **1804**, 76-82 (2010)

turn into homogenous and exponential processes above the glass temperature at 200 K²². From a functional point of view myoglobin is thus dynamically homogeneous at room temperature. Arieh Warshel, co-nobel prize winner in chemistry of 2013, argues that "the complex energy landscape is not the reason of the catalytic power of proteins, flexibility is interfering with rate acceleration, catalysis requires rigid stereo-chemical structures"²³. This applies to the catalytic step specially, since the substrate/product exchange between protein interior and solvent requires a solvent coupled structural flexibility of type II.

13. Curtis, J.E., Tarek, N., Tobias, D.J. Methyl group dynamics as a probe of the protein dynamical transition, *JACS* **126**, 15929 (2004)
14. Bee, M., Quasielastic Neutron Scattering. p. 17, 107-147, 195 Adam Hilger, Bristol, Philadelphia (1988)
15. Squires, G. L. Introduction to the theory of thermal neutron scattering, Dover Books in Physics p. 101 (1978)
16. Cusack, S., Doster, W. Temperature dependence of the low frequency dynamics of myoglobin. *Biophys. J.* **58**, 243-251 (1990)
17. Doster, W. Brownian oscillator analysis of molecular motions in biomolecules in 'Neutron Scattering in Biology, techniques and applications' Eds. Fitter, J., Gutberlet, T., Katsaras, J., Springer, biological and medical physics, biomedical engineering, chapter 20, 461-482 (2006)
18. Doster, W., Diehl, M., Petry, W., Ferrand, M., Elastic resolution spectroscopy: a method to study molecular motions in small biological samples. *Physica B* **301**, 65-68 (2001)
19. Doster, W., Busch, S., Gaspar, A., Appavou, M.S., Wuttke, J., Scheer, J. Dynamical transition of protein hydration water, *Phys. Rev. Lett.* **104**, 098101-4 (2010)
20. Kleinert, Th., Doster, W., Leyser, H., Petry, W., Schwarz, V., Settles, M. Solvent composition and viscosity effects on the kinetics of CO-binding to horse myoglobin. *Biochem.* **37**, 717-733 (1998)
21. Longeville, S., Doster, W. Protein Dynamics and Function in 'Dynamics of Soft Matter, Neutron Applications', Chapter 8, Springer Science (2012)
22. Post, F., Doster, W., Karvounis, G., Settles, M. Structural relaxation and non-exponential kinetic of CO-binding to horse myoglobin. *Biophys. J.* **64**, 1833-1864 (1993)
23. Warshel, A., Bora, R., P., Defining and quantifying the role of dynamics in enzyme catalysis. *J. Chem. Phys.* **144**, 180901-17 (2016)

613
614
615
616
617
618
619
620
621
622
623
624
625
626
627
628
629
630
631
632
633
634
635
636
637
638
639
640
641
642
643
644
645
646
647
648
649
650
651
652
653
654
655
656
657
658
659
660
661
662
663
664
665
666
667
668
669
670
671
672
673
674
675
676
677
678
679
680

Please review all the figures in this paginated PDF and check if the figure size is appropriate to allow reading of the text in the figure.

If readability needs to be improved then resize the figure again in 'Figure sizing' interface of Article Sizing Tool.